# Optimizing Distribution Networks for Cost Minimization

Aditya S Mehta[1]

Electrical Engineering Department, California State University, Los Angeles, USA
Adityamehta9214@gmail.com

**Abstract.** The objective of this paper is the optimisation of distribution networks to minimise loss and operational cost for DSO. The presence of untransposed lines in unbalanced voltages and currents in distribution networks requires an active strategy against negative impacts. In this paper, we use various compensation methods to address the voltage drop in electrical networks. The techniques involve structural methods like network reconfiguration and phase balancing. Automatic voltage regulation using the shunt device and the series device. Local control strategies making use of distributed energy resources are also applied. A new three-phase optimal power flow (OPF) model is proposed using convex optimisation for heavily meshed networks and three-phase inverters with cross-phase capability. The proposed model minimises total costs with simultaneous voltage and current balancing when distributed energy resources are rapidly installed. The proposed method has been confirmed by computational implementation and testing on IEEE test systems.

**Keywords:** Distributed Energy Resources · Electric Vehicle Charge Stations · Cross-phase power flow · Power Quality · Voltage Imbalance Factor

## 1 Introduction

Distribution System Operators (DSOs) aim to reduce losses and costs in distribution network. Because of untransposed lines and one-phase, stochastic generation and loads, the target networks is unbalanced by nature. Unbalanced voltage influences power quality, while unbalanced current causes higher losses. Addressing both challenges represents an important technical challenge.

Sources that are unbalanced can be classified as structural or random. Structural solutions like reconfiguration need more real-time flexibility. Static Transfer Systems (STS) help, but introduce switching transients. The success of converter-based compensation is growing rapidly with the distributed energy resources (DERs) like photovoltaics (PV) and electric vehicle charging station (EVCS).

Research on local control with PVs to mitigate imbalance has been performed but references limited to data available locally. Recent cyber-physical systems allow for system optimisation strategies, which coordinate the distribution of energy resources (DERs) to minimise costs with an imbalance as a secondary objective.


P. Johri et al. (eds.), *Proceedings of the International Conference on Sustainable Computing and Artificial Intelligence (ICSCAI 2025)*, Advances in Engineering Research 298,
https://doi.org/10.2991/978-94-6239-674-6_30

Cross-phase capability of three-phase inverters was largely overlooked in previous works. In particular, this often led to non-convex model formulations, which hindered computational efficiency and scalability. This paper aims to fill these gaps with a new three-phase optimal power flow (OPF) formulation with the following contributions:

- A three-phase OPF model that is convex, polar coordinates, linearized power flow, and a data-driven polynomial approximation of the Voltage Unbalance Factor (VUF). The shape of the network means that optimal solutions can be computed efficiently. Furthermore, the approach scales to large, meshed networks.
- Integrated modelling of three-phase and single-phase EV chargers and PV systems in the OPF to taking full advantage of the capabilities of their devices to improve their performance and avoid harmful conditions.
- By allowing three-phase inverters to operate across phases, the unused capacity of one phase enables more optimisation of the grid conditions and lower costs.

The IEEE 33-bus radial and 192-bus meshed systems were tested on the proposed method. The results give benchmarks to the DSOs to judge: 1. the appropriate compensation to be given to the inverter/load owners of the imbalance, and 2. the justified remuneration to be given for enabling the cross-phase operation.

## 2 Problem Formulation

A convex OPF model is developed in which operational costs are minimised subject to physical and power-quality constraints.

### Power Flow Model

The three-phase power balance equations for bus $i$, phase $\varphi$ are:

$$P^{\varphi}_{i,\mathrm{inj}} + P^{\varphi}_{i,\mathrm{PV}} = P^{\varphi}_{i,\mathrm{ld}} + P^{\varphi}_{i,\mathrm{EV}} + \sum_{j|(i,j)\in L} \sum_{\gamma\in\phi} P^{\varphi\gamma}_{ij} \tag{1}$$

$$Q^{\varphi}_{i,\mathrm{inj}} + Q^{\varphi}_{i,\mathrm{PV}} = Q^{\varphi}_{i,\mathrm{ld}} + Q^{\varphi}_{i,\mathrm{EV}} + \sum_{j|(i,j)\in L} \sum_{\gamma\in\phi} Q^{\varphi\gamma}_{ij} \tag{2}$$

Branch flows $P^{\varphi\gamma}_{ij}, Q^{\varphi\gamma}_{ij}$ are functions of voltages and line impedances. For convexity, a linearized model [1] is extended to three-phase systems, assuming voltages near 1 p.u. and small angle differences. The linearized flows are:

$$P^{\varphi\gamma}_{ij} \approx \hat{P}^{\varphi\gamma}_{ij} = k^{\varphi\gamma}_{1,ij} \frac{V^{\varphi} - V^{\varphi}_{i \quad j}}{x^{\varphi\gamma}_{ij}} + k^{\varphi\gamma}_{2,ij} \frac{\theta^{\varphi} - \theta^{\varphi}_{i \quad j}}{x^{\varphi\gamma}_{ij}} \tag{3}$$

$$Q^{\varphi\gamma} \approx \hat{Q}^{\varphi\gamma} = -k^{\varphi\gamma} \frac{\theta^{\varphi} - \theta^{\varphi}_{i \quad j}}{x^{\varphi\gamma}_{ij}} + k^{\varphi\gamma} \frac{V^{\varphi} - V^{\varphi}_{i \quad j}}{x^{\varphi\gamma}_{ij}}$$

$$ij \qquad ij \qquad 1,ij \; x_{ij}^{\varphi\gamma} \qquad 2,ij \qquad {}_{ij}^{\varphi\gamma} \tag{4}$$

where $k_{1,ij}^{\varphi\gamma}, k_{2,ij}^{\varphi\gamma}$ are constants derived from line parameters.

## Capacity Constraint

Line thermal limits are enforced via a piecewise linear approximation of the apparent power constraint:

$$S_{ij}^{\varphi\varphi} = \sqrt{(P^{\varphi\varphi})_{ij}^2 + (Q^{\varphi\varphi})^2{}_{ij}} \leq S_{ij}^{\max}. \tag{5}$$

Following [2], this is convexified as:

$$\forall h \in \{1, \ldots, H\}, \left[\sin\tfrac{360h}{H} - \sin\tfrac{360(h-1)}{H}\right] P_{ij}^{\varphi\varphi} - \left[\cos\tfrac{360h}{H} - \cos\tfrac{360(h-1)}{H}\right] Q_{ij}^{\varphi\varphi} \leq S_{ij}^{\max} \sin\tfrac{360}{H}. \tag{6}$$

## Voltage Constraints

Voltage magnitudes are bounded:

$$V_{\min} \le V_i^{\varphi} \le V_{\max}. \tag{7}$$

The Voltage Unbalance Factor (VUF) is limited by $\mathrm{VUF}_i \le \mathrm{VUF}_{\max}$. Due to its nonlinearity, a soft quadratic approximation is used within a multi-objective framework:

$$\mathrm{VUF}_i \approx \mathrm{VUF}_i^{\mathrm{apr}} = \sum_{n=0}^{2} \sum_{m=0}^{n} \sum_{\varphi,\gamma \in \phi} \alpha_{imn}^{\varphi\gamma} (V_i^{\varphi})^m (V_i^{\gamma})^{n-m} + \beta_{imn}^{\varphi\gamma} (V_i^{\varphi})^m (\theta_i^{\gamma})^{n-m} + \delta_{imn}^{\varphi\gamma} (\theta_i^{\varphi})^m (\theta_i^{\gamma})^{n-m}. \tag{8}$$

## Objective Function

The primary objective is to minimize operational cost:

$$\min \sum_{s \in S} c_1^s + c_2^s P_{s,\mathrm{inj}}^{\varphi} + c_3^s (P_{s,\mathrm{inj}}^{\varphi})^2 . \tag{9}$$

A multi-objective form incorporating VUF reduction is:

$$\min w' \sum_{s \in S} c_1^s + c_2^s P_{s,\mathrm{inj}}^{\varphi} + c_3^s (P_{s,\mathrm{inj}}^{\varphi})^2 + \sum_{i \in N} w_i \, \mathrm{VUF}_i^{\mathrm{apr}}, \tag{10}$$

where $w', w_i \in [0, 1]$ are weighting factors.

### 2.1 EVCS Models

The distribution network includes modelling of Electric Vehicle Charging Stations (EVCSs) for single-phase and three-phase case studies. In single-phase schemes, the active power of phase $\kappa$ is fixed and determined by scheduled charging, while provision of reactive power support is available at inverter limits. The model of a single-phase EVCS is given.

$$\forall\, i \in N, \quad P^{\kappa}_{i,\mathrm{EV}} = P^{\mathrm{sch}}_{i,\mathrm{EV}}, \tag{11}$$

$$\forall\, i \in N,\ \forall\, \varphi \in \phi,\ \varphi \neq \kappa, \quad P^{\varphi}_{i,\mathrm{EV}} = 0, \tag{12}$$

$$\forall\, i \in N, \quad -\sqrt{\left(S^{\mathrm{inv}}_{i,\mathrm{EV}}\right)^2 - \left(P^{\kappa}_{i,\mathrm{EV}}\right)^2} \leq Q^{\kappa}_{i,\mathrm{EV}} \leq \sqrt{\left(S^{\mathrm{inv}}_{i,\mathrm{EV}}\right)^2 - \left(P^{\kappa}_{i,\mathrm{EV}}\right)^2}. \tag{13}$$

For three-phase EVCS installations, cross-phase active power transfer is permitted. The corresponding formulation is modified as follows:

$$\forall\, i \in N, \quad \sum_{\varphi \in \phi} P^{\varphi}_{i,\mathrm{EV}} = P^{\mathrm{sch}}_{i,\mathrm{EV}}, \tag{14}$$

$$\forall\, i \in N,\ \forall\, \varphi \in \phi, \quad \sqrt{\left(P^{\varphi}_{i,\mathrm{EV}}\right)^2 + \left(Q^{\varphi}_{i,\mathrm{EV}}\right)^2} \leq S^{\mathrm{inv}}_{i,\mathrm{EV}}, \tag{15}$$

$$\begin{aligned} &\forall\, h \in \{1, 2, \ldots, H\},\ \forall\, i \in N,\ \forall\, \varphi \in \phi, \\ &\left(\sin\frac{360^\circ h}{H} - \sin\frac{360^\circ (h-1)}{H}\right) P^{\varphi}_{i,\mathrm{EV}} \\ &\left(-\cos\frac{360^\circ h}{H} - \cos\frac{360^\circ (h-1)}{H}\right) Q^{\varphi}_{i,\mathrm{EV}} \\ &\leq S^{\mathrm{inv}}_{i,\mathrm{EV}} \cdot \sin\frac{360^\circ}{H}. \end{aligned} \tag{16}$$

From the outcome of optimisation, the phase-specific active and reactive power values can be derived with these formulations. It is proven that even when EVCS does not charge, the system can transfer active power between the phases like that of an active power line conditioner [3]. This ability allows for more ancillary services and better economic feasibility.

## 2.2 PV Models

Photovoltaic systems have similar installation methodologies in single-phase as well as three-phase systems in the distribution network. Even though 3-phase PV systems help with voltage and load balancing, uncontrolled single-phase PV systems impact power quality negatively. This requires that PV systems be managed appropriately, to introduce sufficient flexibility for optimalisation as well as meet the power quality requirements.

For single-phase PV installations in phase $\kappa$, the model is defined as

$$\forall\, i \in N, \quad 0 \le P^{\kappa}_{i,\mathrm{PV}} \le P^{\mathrm{sun}}_{i,\mathrm{PV}}, \tag{17}$$

$$\forall\, i \in N,\ \forall\, \varphi \in \phi,\ \varphi \neq \kappa, \quad P^{\varphi}_{i,\mathrm{PV}} = 0, \tag{18}$$

$$\forall\, i \in N, \quad \sqrt{\left(P^{\kappa}_{i,\mathrm{PV}}\right)^2 + \left(Q^{\kappa}_{i,\mathrm{PV}}\right)^2} \le S^{\mathrm{inv}}_{i,\mathrm{PV}}. \tag{19}$$

The nonlinear constraint in (19) is approximated using a piecewise linear method, resulting in

$$\forall\, h \in \{1, 2, \ldots, H\},\ \forall\, i \in N,$$
$$\left(\sin\frac{360^\circ h}{H} - \sin\frac{360^\circ (h-1)}{H}\right) P^{\kappa}_{i,\mathrm{PV}} - \left(\cos\frac{360^\circ h}{H} - \cos\frac{360^\circ (h-1)}{H}\right) Q^{\kappa}_{i,\mathrm{PV}} \le S^{\mathrm{inv}}_{i,\mathrm{PV}} \cdot \sin\frac{360^\circ}{H}. \tag{20}$$

For three-phase PV systems, the following expressions are employed. First, the aggregate active power is bounded by

$$\forall\, i \in N, \quad 0 \le \sum_{\varphi \in \phi} P^{\varphi}_{i,\mathrm{PV}} \le P^{\mathrm{sun}}_{i,\mathrm{PV}}. \tag{21}$$

Then, for each phase, the inverter capacity is constrained by

$$\forall\, i \in N,\ \forall\, \varphi \in \phi, \quad \sqrt{\left(P^{\varphi}_{i,\mathrm{PV}}\right)^2 + \left(Q^{\varphi}_{i,\mathrm{PV}}\right)^2} \le S^{\mathrm{inv}}_{i,\mathrm{PV}}, \tag{22}$$

and the corresponding piecewise linear approximation is given by

$$\forall\, h \in \{1, 2, \ldots, H\},\ \forall\, i \in N,\ \forall\, \varphi \in \phi,$$
$$\left(\sin\frac{360^\circ h}{H} - \sin\frac{360^\circ (h-1)}{H}\right) P^{\varphi}_{i,\mathrm{PV}}$$

$$\left| \cos\left(\frac{360^\circ h}{H}\right) - \cos\left(\frac{360^\circ (h-1)}{H}\right) \right| Q^{\varphi}_{i,\mathrm{PV}} \leq S^{\mathrm{inv}}_{i,\mathrm{PV}} \cdot \sin\left(\frac{360^\circ}{H}\right). \tag{23}$$

In every case, the active and reactive power values of all phases are determined as a result of optimisation. Besides, inverter and network operation limits should not be violated.

Finally, the $P^{\varphi}_{iPV}$ and $Q^{\varphi}_{iPV}$ can be derived as a result of the optimisation problem. To sum up, the QP framework will be the minimisation of the objective function.

# 3 Computational Implementation

## Input Structure and Test Cases

The MATPOWER-based data structure is adapted for three-phase unbalanced networks [4]. Two test systems are employed:

- **IEEE 33-Bus** (12.6kV): Load perturbation alters originally stable balance.
- **192-Bus** (120V): sourced from a heavily meshed, unbalanced IEEE 342 - bus.

The single and three-phase PV and EV Chargers are evaluated at several penetration levels. Parameters Sufficient Are Listed in Table 1.

**Table 1.** System Parameters

| Parameter | 33-Bus | 192-Bus |
|---|---|---|
| Voltage (L-N) | 12.6kV | 120V |
| $V_{\min}/V_{\max}$ (p.u.) | 0.9/1.1 | 0.9/1.1 |
| Cost coeff. $c_1/c_2/c_3$ | 3/0.1/0 | 3/0.1/0 |
| Total load (MW) | 3.75 | 2.9 |
| Total reactive load (MVAR) | 2.3 | 1.82 |
| 3-phase EV capacity (MVA) | 0.54 | 0.12 |
| 3-phase PV capacity (MVA) | 0.9 | 0.3 |
| Slack buses | 1 | 144–192 |

## Method Clustering

Five sub-methods are compared (Table 2):

- *Fixed*: MATPOWER OPF, no cross-phase.
- *OPF*: Linearized OPF (CVX).
- *OPF VUF*: Adds VUF penalty.
- *Crossphase*: Enables cross-phase operation.
- *Crossphase VUF*: Combines cross-phase and VUF penalty.

Simulations run in MATLAB 2022a on an Intel i5-8250U with 8GB RAM.

**Table 2.** Sub-Methods for Ablation Study

| Sub-Method | Solver | Key Equations |
|---|---|---|
| Fixed | MATPOWER | (1-4),(13),(15),(19),(21),(23),(27),(29) |
| OPF | CVX | (5-12),(14-15),(19),(21),(23),(27),(30) |
| OPF VUF | CVX | (5-12),(14-15),(18),(20-21),(23),(27),(30) |
| Crossphase | CVX | (5-12),(14-15),(19),(21-24),(26-28),(30-31),(33) |
| Crossphase VUF | CVX | (5-12),(14-15),(18),(20-24),(26-28),(30-31),(33) |

### Operating Scenarios

Four main scenarios are defined (all with/without cross-phase capability):

- *Base(NC)*: No PV/EV.
- *PV-noon(NC)*: High PV generation.
- *EV-night(NC)*: High EV charging.
- *PV-EV-Afternoon*: Combined PV/EV.

Each scenario is divided into eight time intervals with linearly increasing load unbalance.

## 4 Parameter Tuning

### VUF Quadratic Regression

Coefficients $\alpha, \beta, \delta$ in the VUF approximation are obtained via multivariable quadratic regression over voltage magnitude (0.9–1.1 p.u.) and angle ($-5^\circ$–$5^\circ$). Quadratic regression outperforms linear and is adopted.

### Pareto Front Trade-Off

A Pareto analysis shows the cost-VUF trade-off for *Crossphase VUF*. Weight $w = 0.1$ gives significant VUF reduction with moderate cost increase.

## 5 Results and Discussion

### Total Cost Analysis

Table 3 shows total cost for the *PV-EV-Afternoon* simulate (5). Cross-phase techniques help in reducing overall cost through effective utilisation of inverter capacity. VUF penalty raises an expense a little. Savings in Costs are more in the radial 33-Bus system as compared to the meshed 192-Bus system.

**Table 3.** Total Cost for *PV-EV-Afternoon* Scenario (Interval 5)

| System | Fixed | OPF | OPF-VUF | Crossphase | Crossphase-VUF |
|---|---|---|---|---|---|
| 33-Bus | 346.54 | 346.54 | 351.72 | 341.29 | 344.55 |
| 192-Bus | 127.19 | 127.19 | 147.22 | 127.19 | 142.07 |

**Table 4.** Total Cost for Different Scenarios (Interval5)

| | Base | | EV-Night | | PV-Noon | |
|---|---|---|---|---|---|---|
| System | (C) | (NC) | (C) | (NC) | (C) | (NC) |
| 33-Bus | 361.87 | 367.81 | 369.94 | 373.40 | 337.35 | 339.27 |
| 192-Bus | 155.19 | 155.19 | 171.19 | 171.19 | 126.94 | 129.92 |

### Voltage Unbalance Analysis

Figures 1 and 2 show VUF across all intervals. *Crossphase VUF* results in the biggest drops. While cross-phase alone enhances VUF, incorporating the explicit VUF penalty yields additional progress. PVs produce more unbalanced reduction than EVs. Once more, benefits are larger in the radial 33-Bus configuration.

Table 6 (worst-case interval 8) confirms that cross-phase operation significantly alleviates unbalance, though the strict VUF limit is not fully met under extreme conditions.

**Table 5.** VUF Summary for Worst-Case Interval (8)

| | Base | | EV-Night | | PV-Noon | |
|---|---|---|---|---|---|---|
| System | (C) | (NC) | (C) | (NC) | (C) | (NC) |
| 33-Bus | 0.018 | 0.025 | 0.021 | 0.028 | 0.015 | 0.022 |
| 192-Bus | 0.032 | 0.032 | 0.035 | 0.035 | 0.028 | 0.030 |

## 5.1 Total Power Loss of the Test Systems

The overall power losses incurred by the test systems under various dispatch strategies are detailed in Tables 7 and 8. An examination of Table 7. The results suggest that the total power loss in the IEEE 33-Bus system increases as the load imbalance severity increases. Considering that the power of the three-phase load is constant in all intervals, the increase in losses is due to the increase in line imbalance. The cross-phase operation is implemented to achieve cost and VUF minimisation; however, in doing so, two forms may arise.:

[label=(i)]

1. When the load demand is unbalanced, inverter power is allocated to locally compensate for a line imbalance on the lower side and improve balance on the upper main line. This solution is effective in radial configurations.

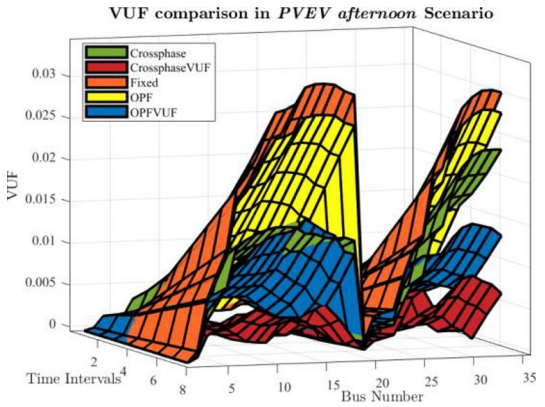


**Fig. 1.** VUF Comparison of sub-methods in *PVEV afternoon* scenario in 33 bus system

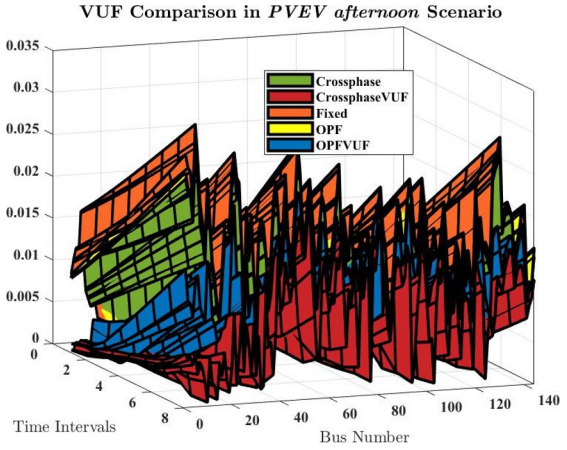


**Fig. 2.** VUF Comparison of sub-methods in *PVEV afternoon* scenario in 192 bus system (Slack buses are not shown)

**Table 6.** Percentage of buses violating the IEEE 1159 standard in different scenarios (%).

| | **Base** | | **PV-Noon** | | **EV-Night** | |
|---|---|---|---|---|---|---|
| **System** | (NC) | (C) | (NC) | (C) | (NC) | (C) |
| 33-Bus | 76 | 0 | 24 | 6 | 69 | 0 |
| 342-Bus | 75 | 43 | 46 | 41 | 71 | 44 |

2. Moving the active power, that can be produced by single-phase PV units, from one phase to another. This plan uses available line capacity to feed power to upper side loads or loads in odd phases. However, this does not guarantee balancing of the upper main line every time.

Considering these factors, Table 7 shows that when the loads are roughly balanced (time intervals 1–3), the *Crossphase VUF* the method makes a trade-off by slightly compromising line imbalance and the associated losses to gain improved VUF and cost performance. On the other hand, in very unbalanced conditions, the *Crossphase VUF* approach reduces both losses and cost without compromising VUF. Consequently, both current and voltage imbalances reduce together with cost savings under these conditions. A related evaluation of Table 8. The heavily meshed grid shows losses connected with the shown in the *Crossphase VUF* approach exceed those of the *Crossphase*. In other words, the line imbalance has to be compromised in meshed networks in every time period to improve VUF. This observation proves that even if voltage and current might be out of proportion, they don't always necessarily behave in a directly proportional way.

The outcomes from the scenario are recapped in Tables 9 and 10. The contribution of EVs and PVs during off-peak hours in the IEEE 33-Bus system always helps in reducing losses in all time intervals. This shows the benefits of cross-phasing with radial topology. Moreover, there are the following important points.:

- A comparison between *Base (NC)* and *Base (C)* Single-phase generation during interval 1 is absent. This implies a reduction in VUF, and cost could induce line imbalance in a meshed network. It appears that meshed grids may not entirely reap the benefits generated by the first form of cross-phasing.
- When comparing *EV-Night (NC)* with *EV-Night (C)*, in areas where cross-phasing is mostly caused by PVs, and there is substantial single-phase generation, loss reduction does not occur until around interval 7, which provides evidence for the second type of cross-phasing. comparison of the PV Noon (NC) *PV-Noon (C)*. Only inter-phase traffic of electric vehicles will produce the same outcome on loss reduction during all intervals when the park values are on.

## 6 Conclusion

A three-phase optimal power flow formulation has been suggested recently that considers both voltage angles and voltage magnitudes (AC load flow) for calculation for meshed networks. In this formulation, the optimal control of active and reactive power set points in each phase is enabled for both single-phase and three-phase PV systems and EV chargers. Including voltage angles and magnitudes allows the incorporation of the voltage unbalance factor (VUF) as a constraint or objective. In a bid to enhance the computability of equations and constraints, all constraints have been linearized and the VUF constraint has been

**Table 7.** Total Power Loss in the IEEE 33-Bus System for Various Dispatch Methods (kW)

| Hour | Fixed | OPF | OPF-VUF | Crossphase | Crossphase-VUF |
|---|---|---|---|---|---|
| 1 | 4.88 | 4.87 | 4.68 | 4.86 | 5.01 |
| 2 | 4.98 | 4.97 | 4.81 | 4.92 | 5.05 |
| 3 | 5.15 | 5.14 | 5.13 | 5.06 | 5.16 |
| 4 | 5.39 | 5.37 | 5.35 | 5.26 | 5.32 |
| 5 | 5.70 | 5.69 | 5.60 | 5.54 | 5.56 |
| 6 | 6.08 | 6.07 | 5.91 | 5.88 | 5.86 |
| 7 | 6.53 | 6.52 | 6.29 | 6.29 | 6.22 |
| 8 | 7.06 | 7.04 | 6.75 | 6.78 | 6.66 |

**Table 8.** Total Power Loss in the IEEE 192-Bus System for Various Dispatch Methods (kW)

| Hour | Fixed | OPF | OPF-VUF | Crossphase | Crossphase-VUF |
|---|---|---|---|---|---|
| 1 | 14.15 | 14.40 | 15.51 | 14.42 | 14.80 |
| 2 | 14.47 | 14.72 | 16.11 | 14.72 | 14.82 |
| 3 | 15.00 | 15.25 | 16.62 | 15.24 | 15.14 |
| 4 | 15.74 | 16.00 | 17.16 | 15.95 | 15.99 |
| 5 | 16.70 | 16.94 | 17.85 | 16.86 | 17.29 |
| 6 | 17.87 | 18.07 | 18.72 | 17.92 | 18.53 |
| 7 | 19.25 | 19.43 | 19.81 | 19.29 | 19.79 |
| 8 | 20.85 | 21.00 | 21.09 | 20.81 | 20.97 |

**Table 9.** Total Power Loss of the 33-Bus System with the Crossphase-VUF Method under Different Scenarios (kW)

| Hour | 1 | 2 | 3 | 4 | 5 | 6 | 7 | 8 |
|---|---|---|---|---|---|---|---|---|
| Base (C) | 5.22 | 5.20 | 5.09 | 5.37 | 5.69 | 5.83 | 5.98 | 6.11 |
| Base (NC) | 5.31 | 5.41 | 5.59 | 5.83 | 6.15 | 6.53 | 6.99 | 7.51 |
| EV-Night (C) | 5.87 | 5.74 | 5.66 | 5.78 | 6.31 | 6.66 | 6.49 | 6.76 |
| EV-Night (NC) | 6.27 | 6.06 | 6.03 | 6.17 | 6.38 | 6.66 | 7.01 | 7.40 |
| PV-Noon (C) | 2.43 | 2.68 | 3.12 | 3.35 | 3.32 | 3.07 | 3.89 | 4.48 |
| PV-Noon (NC) | 2.80 | 2.79 | 2.85 | 2.96 | 3.23 | 3.67 | 4.46 | 5.06 |

approximated using a second-degree multivariable polynomial. This polynomial was calculated over a wide dataset comprising data from the entire operational range of voltage magnitudes.

**Table 10.** Total Power Loss of the 192-Bus System with the Crossphase-VUF Method in Different Scenarios (kW)

| **Hour** | 1 | 2 | 3 | 4 | 5 | 6 | 7 | 8 |
|---|---|---|---|---|---|---|---|---|
| Base (C) | 16.72 | 16.85 | 17.17 | 17.79 | 18.53 | 19.35 | 20.31 | 21.38 |
| Base (NC) | 16.48 | 16.79 | 17.32 | 18.06 | 19.00 | 20.16 | 21.53 | 23.11 |
| EV-Night (C) | 19.85 | 20.02 | 20.38 | 21.01 | 21.77 | 22.64 | 23.57 | 24.69 |
| EV-Night (NC) | 19.60 | 19.77 | 20.17 | 20.79 | 21.59 | 22.58 | 23.77 | 25.18 |
| PV-Noon (C) | 12.52 | 12.70 | 12.98 | 13.64 | 14.93 | 16.12 | 17.30 | 18.46 |
| PV-Noon (NC) | 12.68 | 12.87 | 13.32 | 14.24 | 15.68 | 16.97 | 18.40 | 19.77 |

## References

1. H. Yuan, F. Li, Y. Wei, and J. Zhu, "Novel linearized power flow and linearized opf models for active distribution networks with application in distribution lmp," *IEEE Transactions on Smart Grid*, vol. 9, no. 1, pp. 438–448, 2016.
2. T. Akbari and M. T. Bina, "Linear approximated formulation of ac optimal power flow using binary discretisation," *IET Generation, Transmission & Distribution*, vol. 10, no. 5, pp. 1117–1123, 2016.
3. P. Salmero´n, J. Montano, J. Va´zquez, J. Prieto, and A. P´erez, "Compensation in nonsinusoidal, unbalanced three-phase four-wire systems with active power-line conditioner," *IEEE transactions on power delivery*, vol. 19, no. 4, pp. 1968–1974, 2004.
4. R. D. Zimmerman, C. E. Murillo-Sa´nchez, and R. J. Thomas, "Matpower: Steady-state operations, planning, and analysis tools for power systems research and education," *IEEE Transactions on power systems*, vol. 26, no. 1, pp. 12–19, 2010.